

ROBUSTNESS OF SIDE SLIP ESTIMATION AND CONTROL ALGORITHMS FOR VEHICLE CHASSIS CONTROL

Aleksander Hac
Edward Bedner
Delphi Corporation
United States of America
Paper Number 07-0353

ABSTRACT

A process of evaluating robustness of the side slip angle estimation and control algorithms for vehicle dynamics control is described and selected results are presented. The estimation algorithm is a non-linear observer with adaptation to road friction and a compensation for a road bank angle. The estimator relies on the information from the sensors and other estimates, on a nominal model of vehicle, and on assumptions about disturbances, all of which may be inaccurate. In order to evaluate the effects of these errors on the estimation of side slip angle, a systematic robustness study is performed. It uses analysis, vehicle testing and simulations based on a validated vehicle model. First, the effects of single factors in various maneuvers and road conditions are examined and those having the largest contributions to errors are identified. Subsequently, the combinations of multiple error factors are studied, with the emphasis on the worst possible combinations. The robustness of the control system is then evaluated along the same lines, with the particular emphasis on the worst case scenarios, when the side slip angle estimates are the least accurate.

INTRODUCTION

Accurate information about the side slip angles of vehicle and tires is critical in controlling vehicle motion in the yaw plane using active chassis systems, such as brake-based Electronic Stability Control (ESC) systems and active front or rear steering systems. Excessive slip angle of the vehicle and the rear axle generally indicates an oversteer condition and may lead to the loss of directional control of vehicle. It also increases the risk of tripped rollover, especially when the lateral velocity exceeds critical sliding velocity (i.e. a minimal lateral velocity, which is sufficient for the vehicle to roll over upon tripping). A large slip angle of front tires makes the vehicle insensitive to minor steering corrections and

reduces the effect of brake intervention at a specified slip level on vehicle yaw moment.

Since the side slip angle cannot be easily measured, it must be estimated using available sensors and possibly knowledge of vehicle parameters. A typical sensor set available in vehicles equipped with ESC systems includes steering angle sensor, yaw rate sensor, lateral acceleration sensor, and four wheel speed sensors, from which vehicle longitudinal speed is derived. A number of algorithms for estimating the side slip velocity and side slip angle using this sensor set have been proposed. They can be roughly classified into four categories: 1) estimators relying on kinematic relationships such as pseudo-integrator, e.g. [1]; 2) estimators based on algebraic equations [2], 3) estimators based on a dynamic model such as Kalman filter [3, 5], and 4) other methods, for example neural networks [4] or fuzzy logic.

The model based approach is the most common. It has the best potential since it uses all available information including the sensor data and the knowledge of vehicle dynamics represented in the model with specific parameters. The disadvantage is that the accuracy of estimates is affected not only by the sensor errors and unknown disturbances, but also by the mismatch between the model and the actual vehicle. Since the estimate of side slip angle is used in vehicle stability control system [3, 6], the estimation errors affect vehicle performance. Consequently, robustness of the algorithms must be carefully evaluated before introducing the system in production vehicles. To the best knowledge of the authors, no comprehensive robustness analysis of side slip angle estimation and control algorithms has been described in literature.

In this paper a process of evaluating robustness of the side slip angle estimation and control algorithms for vehicle dynamics control is described and selected results are presented. The estimation algorithm is a non-linear observer with adaptation to

road friction and a compensation for a road bank angle. The control algorithm combines tracking of the desired yaw rate with regulation of the rear axle side slip angle, which must be kept within limits necessary for maintaining vehicle stability and maneuverability. Since both the estimation and control algorithms are nonlinear, their robustness properties depend on operating point, types of driver inputs, sensor errors, road conditions, etc. Consequently, it is virtually impossible to analytically establish global conditions of stability and robustness. A systematic robustness study is therefore performed. It uses analysis, vehicle testing, and simulations based on a validated vehicle model. First, the effects of single factors in various maneuvers are examined and those having the largest contributions to errors are identified. Subsequently, the combinations of multiple error factors are studied, with the emphasis on the worst possible combinations.

CONTROL SYSTEM OVERVIEW

This section discusses the design of the entire control system, which includes the estimation algorithm along with other elements. The relationship of the control system elements is depicted in the block diagram representation of Figure 1.

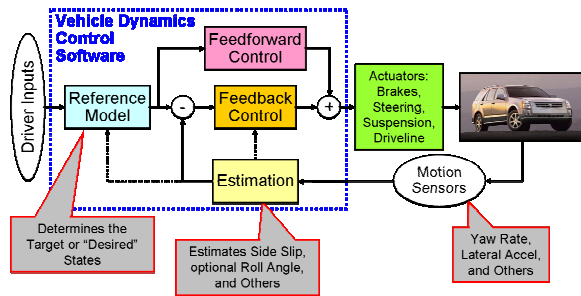


Figure 1. Functional diagram of the control system

The intent of the control system is to enhance the handling characteristics of the vehicle, especially during critical driving situations. One of the design goals is to maintain a stable directional response of the vehicle, meaning that the vehicle's side slip angle and roll angle are not excessive, thus striving to avoid spin-outs and rollovers. A second design goal is to try to track (follow) the driver's intended path or rotation, which is discernable from the driver's inputs of steering, braking, and throttle. Excessive deviations from the target path or excessive side slip or roll angle are counteracted through actuation of one or more active systems, which may include

brakes, steering, suspension, or drivetrain systems. In this work, the main actuation is with an active brake system commonly referred to as Electronic Stability Control (ESC), in combination with engine torque regulation capability.

The chosen control system structure is a model-reference approach that is designed to track a desired value of yaw rate while also keeping the vehicle side slip angle and roll angle within limits necessary for maintaining vehicle yaw and roll stability. As shown in Figure 1, the elements of the control system are:

- Sensors for monitoring vehicle motion and for monitoring driver inputs
- Actuators to influence tire forces (specifically an active brake system) and thereby influence vehicle motion
- Software code implementation of algorithm functions for a state estimator, a reference model, feedback control, and feed-forward control, which are further explained below

The *state estimator* generates the estimates of variables which cannot be measured directly at acceptable cost, but are important for the control algorithm. The estimated variables include vehicle speed, surface coefficient of friction, vehicle and tire side slip angles, and road bank angle. This process will be described in detail in subsequent sections. Vehicle roll angle relative to the road surface can also be estimated within this block.

The *reference model* generates the desired response of the vehicle in terms of the yaw rate, which represents the driver's intention and should be tracked by the vehicle, except when the vehicle is in danger of losing stability in yaw or roll planes. The primary signals used are the hand wheel angle and vehicle speed, which is estimated from wheel speed sensors. In addition, the bank angle estimate and the surface friction estimate are utilized. The first one is used to compensate the desired yaw rate for the bank angle of the road, the second to limit the desired yaw rate depending on road friction.

The vehicle level *feedback control* includes closed loop control of vehicle yaw rate and side slip angle. The output control signal is the corrective yaw moment. It is determined to provide a proper balance between the yaw response and stability. When the side slip angle is small, tracking the desired yaw rate is the primary goal of control. The

emphasis shifts to control of the side slip angle if its magnitude and/or rate of change become excessive. Conceptually, the control law can be described by the following equation.

$$\begin{aligned} \Delta M_z = & (1-w)[K_{\Omega p}(\Omega_d - \Omega) + K_{\Omega d}(\dot{\Omega}_d - \dot{\Omega})] \\ & + w(K_{\beta p}\beta_r + K_{\beta d}\dot{\beta}_r) \end{aligned} \quad (1).$$

Here ΔM_z is the desired change in the yaw moment due to feedback correction, Ω_d and Ω are the desired and measured yaw rates, β_r is the rear axle slip angle and symbols $K_{\Omega p}$, $K_{\Omega d}$, $K_{\beta p}$, and $K_{\beta d}$ are the proportional (P) and derivative (D) gains on yaw rate and side slip angle and w is a weighting factor. The control law (1) represents a combination of PD tracking control of yaw rate and PD regulation of the side slip angle of the rear axle. The latter is the most direct indicator of vehicle stability in the yaw plane. The control gains are adapted to vehicle speed and surface coefficient of friction. For example, side slip angle gains increase with increasing vehicle speed and as surface becomes more slippery.

The weighting factor w , which determines the balance between the yaw rate tracking and side slip control depends primary on a term combining the estimated rear axle side slip angle and its derivative. When this term is below a first threshold value, then $w = 0$ and only yaw rate tracking control is performed. When it is above a second larger threshold, then $w = 1$ and only side slip angle control is performed. When the term is between the two thresholds, the weighting factor is assigned a proportionate value between 0 and 1. In this case, both feedback control terms (yaw rate tracking and side slip regulation) are used with appropriate weighting. The thresholds depend on the surface coefficient of friction and vehicle speed. In effect, this logic gives more emphasis to side slip control when the rear side slip angle is large or is becoming large, and more emphasis to yaw rate when side slip angle is small. The weighting function is continuous, thus providing a smooth blending of control terms.

In addition, the side slip angle control term is gradually attenuated when bank angle increases beyond a specified threshold. This is done in order to improve robustness of the control algorithm on large banks. Since driving on large banks does not occur often and very large bank angles may occur only on roads with high coefficient of friction, where yaw rate control is quite effective, this is an acceptable compromise.

The *feed-forward control* generates control actions which depend primarily on the driver input signals (e.g. handwheel angle, brake pedal force) and vehicle

speed, but do not depend on the response of vehicle measured by inertial sensors. One example of feed-forward control is the rollover mitigating intervention in dynamic maneuvers (e.g. NHTSA's "fishhook" road edge recovery maneuver [7]) which aims at preventing the loss of vehicle stability caused by large and rapid driver's steering inputs.

The outputs of both the *feed-forward* and *feedback* control blocks are the corrective yaw moments and they are combined into one total yaw moment command. The total yaw moment command is an input to the *actuator control* function. In this function, the wheels to which active braking is applied are determined, and the desired level of brake force or change in wheel velocity for each wheel is determined to generate the desired yaw moment. Since the sensitivity of vehicle yaw moment to changes in brake slip depends on the operating point of the vehicle and tires, the knowledge of tire slip angle and surface friction is very helpful in this determination. A tracking control is used to regulate wheel brake pressure such that the actual wheel slip tracks the desired wheel slip. Finally, the actuator control is activated only when certain conditions are satisfied in order to prevent the frequent activations of the brake system in response to very small errors. In effect, control is disabled when the total corrective moment is small in magnitude.

SIDE SLIP ESTIMATION ALGORITHM OVERVIEW

In this section the side slip angle estimation algorithm is briefly described. Since the main purpose here is to develop an understanding of how the sensor errors, parameter variations, changes in road friction, etc., affect the side slip estimates and consequently the control of the vehicle, only a simplified version of the algorithm is presented. Certain details not instrumental to achieving this goal have been omitted in the interest of brevity and clarity.

Several approaches to the estimation of vehicle side slip angle have been initially developed and evaluated in simulation and vehicle testing. They included: 1) an estimator using a kinematic relationship between lateral acceleration, derivative of lateral velocity, yaw rate and vehicle speed to obtain an estimate of lateral velocity through pseudo-integration, 2) an estimator based on algebraic equations derived from a linear bicycle model of vehicle and the parametric adaptation of cornering

stiffness coefficients, 3) an observer based on a linear dynamic bicycle model and parameter adaptation, 4) an observer based on a two-track model of vehicle and estimated longitudinal forces from tire brake pressures, 5) a reduced-order observer based on a non-linear bicycle model and empirically-determined tire lateral force characteristics. The last approach proved to yield the most consistent performance and used only readily available measurements, hence it was selected.

There are several difficulties in designing a robust observer of vehicle side slip angle, which can provide good estimates over the entire operating range. The most fundamental difficulty is the trade off between the tracking performance and robustness to errors and other variations. In order to be robust, the observer must be stable. Vehicle behavior, however, can become marginally stable or unstable under certain conditions. Since the response of an unstable system cannot be tracked precisely by a stable observer, a possibility exists that very large side slip angle may be underestimated if a level of robustness is to be achieved. This trade-off is acceptable, since with the ESC system enabled, very large slip angles will be achieved only in extremely rare circumstances and the full control authority will be directed at reducing the side slip angle after it exceeds a certain threshold, regardless of its magnitude.

When vehicle is near or at the limit of adhesion, tire forces and consequently yaw dynamics, depend strongly on surface coefficient of friction. For example, limit tire forces on ice can be about ten times smaller than on dry surface. The vehicle model used within the observer should therefore be adapted to the changing surface friction. The coefficient of friction, however, is unknown and has to be estimated. Thus the estimation of side slip angle depends on another estimate, which increases the potential for errors. In addition, the effect of road bank angle on the measured lateral acceleration is similar to the effect of changes in lateral velocity of vehicle. Consequently, estimating bank angle which, with the given set of sensors, cannot be made completely independent of estimating side slip velocity, is helpful in estimating lateral velocity. Longitudinal velocity of vehicle, which is estimated primarily from wheel speed sensors, is also used in the estimation of slip angle. These influences are illustrated in Figure 2.

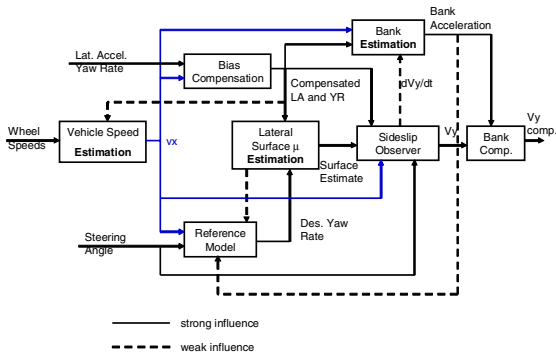


Figure 2. Signal flow within the side slip estimation algorithm.

In addition to directly measured variables of steering angle and yaw rate, the side slip angle estimator uses estimated vehicle speed, surface coefficient of friction and the estimated road bank acceleration (i.e. bank angle).

The estimator of side slip velocity used in this paper is derived from a non-linear single track model of vehicle. Combining the equation expressing the second law of dynamics for lateral forces:

$$Ma_y = F_{yf} \cos \delta_f + F_{yr} \quad (2).$$

with the kinematic relationship

$$a_y = \dot{v}_y + v_x \Omega \quad (3).$$

yields the following equation

$$\dot{v}_y = -v_x \Omega + \frac{F_{yf} \cos \delta_f + F_{yr}}{M} \quad (4).$$

Here M is vehicle mass, a_y is lateral acceleration, F_{yf} is the lateral tire force sum for the two front tires, F_{yr} is the lateral tire force sum for the two rear tires, δ_f is the front wheel steering angle, v_y denotes the lateral velocity at the vehicle center of gravity, v_x is the longitudinal velocity, and Ω is vehicle yaw rate. Equation (4) is the key equation describing the vehicle lateral dynamics. A critical step in constructing an observer is modeling of lateral tire forces per axle, F_{yf} and F_{yr} . They depend primarily on the tire slip angle and surface coefficient of adhesion. The tire lateral force characteristics used in the observer are determined empirically. First, the steady-state characteristics on two extreme surfaces,

dry concrete and ice, are determined once per vehicle by testing the vehicle under nominal load conditions in approximately steady-state maneuvers performed on level surfaces. These two characteristics form an envelope containing all others. An example plot of the tire lateral force per axle determined from the test data on dry surface is shown in Figure 3.

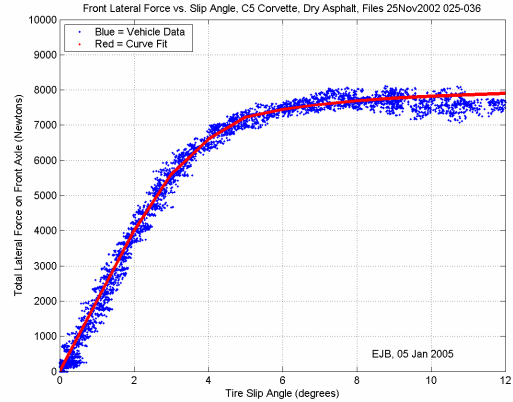


Figure 3. Example lateral tire force per axle determined from test data.

The estimates of actual forces are then determined within the estimation algorithm through interpolation based on the estimated surface coefficient of friction in lateral direction. This process is illustrated in Figure 4 where the index i refers to either front or rear axle.

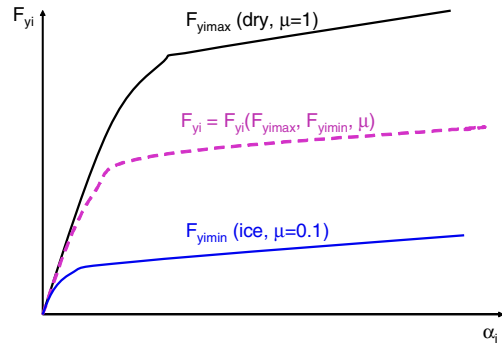


Figure 4. Example axle lateral force characteristics.

The lateral force for any surface friction, μ , is determined in real time by interpolating between the two extreme characteristics obtained for μ_{dry} (typically 1.0) and μ_{ice} (typically 0.1). That is

$$F_{yi}(\alpha_i, \mu) = F_{yi \max}(\alpha_i) \frac{\mu - \mu_{ice}}{\mu_{dry} - \mu_{ice}} \quad \hat{\mu} = \frac{|a_y|}{a_{y \max}} \quad (10).$$

$$+ F_{yi \min}(\alpha_i) \frac{\mu_{dry} - \mu}{\mu_{dry} - \mu_{ice}}$$

(5).

Once these forces are determined, the estimate of vehicle lateral velocity, v_y , can be computed from equation (5), since other variables (v_x , Ω and δ_f) and the parameter M on the right side of equation (5) are known. When the lateral velocity, v_y , is determined, then the vehicle side slip angle, β , and the front and rear tire side slip angles, α_f and α_r , can be computed from the known kinematic relationships. This yields the following set of equations for the observer

$$\dot{\hat{v}}_y = -\hat{v}_x \Omega + \frac{\hat{F}_{yf}(\hat{\alpha}_f, \hat{\mu}) \cos \delta_f + \hat{F}_{yr}(\hat{\alpha}_r, \hat{\mu})}{M} \quad (6).$$

$$\hat{\alpha}_f = \tan^{-1} \frac{\hat{v}_y + a \Omega}{\hat{v}_x} - \delta_f \quad (7).$$

$$\hat{\alpha}_r = \tan^{-1} \frac{\hat{v}_y - b \Omega}{\hat{v}_x} \quad (8).$$

$$\hat{\beta} = \tan^{-1} \frac{\hat{v}_y}{\hat{v}_x} \quad (9).$$

In the above equations, hats denote estimated variables, and a and b are the distances of the vehicle center of gravity to the front and rear axles, respectively. In practice, the differential equation (6) is replaced by a discrete time counterpart, from which the lateral velocity estimate, \hat{v}_y , at any time instant is determined using the estimate from the previous iteration. The tire slip angles used in equation (6) are obtained from the previous iteration. The estimated lateral axle forces are determined from equation (5), in which the unknown surface friction coefficient and slip angles are replaced by the estimated values.

The estimate of surface friction is determined primarily from lateral acceleration. When the vehicle is at or near the friction limit and approximately in a steady-state turn, the surface estimate can be determined from

Here $a_{y \max}$ is the maximum lateral acceleration, which vehicle can develop on dry, level surface in a steady-state turn. More specifically, the surface estimator uses three sets of conditions:

entry conditions – vehicle is at or near the limit of adhesion and approximately at steady-state. The surface estimate is determined from equation (10);

exit conditions – vehicle is in the linear range of handling, in which case the estimate is set at the default value of 1;

hold conditions – when neither entry nor exit conditions are satisfied. The most recent estimate is held.

The above conditions are determined using the desired and measured yaw rate and measured lateral acceleration, in particular the magnitudes of yaw rate error (the difference between the desired and measured yaw rate) and the magnitude of the derivative of lateral acceleration. Note that effectively the surface is not estimated when the vehicle is in the linear range of handling. In this case, however, the lateral forces are nearly independent of surface friction.

The observer based on equations (5) through (9) is a reduced order observer. A full order observer, which includes the yaw moment equation in addition to the lateral force equation, has been investigated, but did not offer improved performance, since the yaw rate signal is quite accurate. The observer as illustrated in Figure 2 includes bank effect compensation. This feature of the algorithm is discussed in the next section.

SIDE SLIP ESTIMATION ROBUSTNESS

The observer described in the previous section relies on several simplifying assumptions, knowledge of vehicle parameters and information from sensors, all of which may be inaccurate. More specifically, the observer uses the following information, which affects the estimates:

1) Variables obtained directly or indirectly from sensors. These include:

- directly measured yaw rate Ω ;

- vehicle longitudinal speed, v_x , which is estimated primarily from 4 wheel speeds;
- front wheel steering angle, δ_f , which is obtained from measured hand wheel angle;
- lateral acceleration, a_y , affecting the estimate of slip angle indirectly through the surface estimate.

2) Vehicle parameters:

- vehicle mass, M ,
- load distribution between front and rear axles expressed by the distances a and b from the center of gravity to front and rear axles, respectively,
- tire lateral force characteristics

3) Assumptions inherent in the bicycle model

- the road is level (no bank or inclination),
- no disturbances in the form of lateral forces or yaw moments are considered explicitly,
- lateral forces per axle are not affected by braking or tractive forces or by changes in vertical force.

As illustrated in Figure 2, many of the error-contributing factors described above, for example sensor bias and road bank angle, are reduced through compensation algorithms. Disturbances in the form of lateral forces and moments and the changes in lateral forces due to longitudinal forces, even though are not explicitly considered, affect the measured yaw rate and lateral acceleration signals, which reduces sensitivity of estimates to these disturbances.

Robustness of the estimation algorithm has been evaluated via analysis, testing and simulations. Each one of these methods has its strengths and weaknesses. Analysis is limited to simplified models, but provides general insights into the predicted direction and often magnitudes of the estimation errors resulting from particular influences, which apply to all vehicles. Vehicle testing was used for three major purposes: 1) to generate the data necessary to validate the vehicle model used in simulation; 2) for the initial evaluation of the algorithm performance in real world conditions and to uncover potential weaknesses; 3) to estimate the range of errors in some variables, which are difficult to model. An example is the error in vehicle speed, which is estimated from wheel speeds. Simulation performed with a validated vehicle model permits the

most comprehensive evaluation of algorithm robustness. The sensor errors, parameter variations and disturbances in the form of road inclinations, braking forces, etc. can be modeled with relative ease and included in simulation scenarios. Maneuvers, which may be difficult or dangerous to perform, can be simulated without risk. In what follows, each of these three methods of evaluation is illustrated using examples due to space limitation.

Analysis

Analysis using simplified models has been used to provide better understating of propagation of errors within the algorithm, to estimate the magnitudes of errors in side slip estimation resulting from sensor errors, parameter variations and disturbances, and to determine the direction of these influences. The analytical method is illustrated here using an example of bank angle. The results of this analysis suggest a method of compensating for a bank angle. Similar analysis has been performed regarding other error factors.

The presence of bank angle, ϕ , and the associated gravity component, $g \sin \phi$, affects directly the equation (4) expressing the balance of lateral forces. Consequently, in presence of bank this equation becomes

$$\dot{v}_y = -v_x \Omega + \frac{F_{yf} \cos \delta_f + F_{yr}}{M} + g \sin \phi \quad (11).$$

In the observer equation (6), in contrast, the bank acceleration component is disregarded. Consequently, in the presence of bank angle the estimate of lateral velocity is biased. The amount of bias can be determined during driving in the linear handling range. In this case the lateral axle forces are

$$F_{yf} = -C_f \alpha_f = -C_f \left(\frac{v_y + a\Omega}{v_x} - \delta_f \right) \quad (12a).$$

$$F_{yr} = -C_r \alpha_r = -C_r \frac{v_y + a\Omega}{v_x} \quad (12b).$$

Here C_f and C_r denote the cornering stiffness values for both tires of the front and rear axle, respectively. Analogous equations hold for the estimated lateral forces \hat{F}_{yf} and \hat{F}_{yr} using the estimated lateral velocity, \hat{v}_y . Substituting these into equations (11)

and (6) and subtracting on both sides yields the following differential equation for the estimation error:

$$\dot{e}_{vy} = -\frac{C_f + C_r}{Mv_x} e_{vy} - g \sin \phi \quad (13).$$

Here e_{vy} is the lateral velocity estimation error, which is defined as a difference between the estimated and actual lateral velocity

$$e_{vy} = \hat{v}_y - v_y \quad (14).$$

Consequently, the steady-state errors in side slip velocity, e_{vyss} and side slip angle, $e_{\beta ss}$, are

$$e_{vyss} = -\frac{Mv_x}{C_f + C_r} g \sin \phi \quad (15).$$

$$e_{\beta ss} = -\frac{M}{C_f + C_r} g \sin \phi \quad (16).$$

The estimation errors caused by the bank angle depend on the values of cornering stiffness per axle, which vary with operating point of vehicle and are generally smaller in the non-linear handling range than during normal driving. However, the sum of cornering stiffness values is always positive, so the sign of errors can be predicted. Knowing the range of values for $C_f + C_r$ the range of magnitude of errors can be estimated.

The road bank angle is a significant contributor to the error in side slip estimation, but it is partially compensated for in the algorithm. This is done as follows. First, an estimate of the bank angle is obtained. Since the measured lateral acceleration, a_{ym} , includes the component of gravity due to the bank angle, ϕ , it is given by

$$a_{ym} = \dot{v}_y + v_x \Omega - g \sin \phi \quad (17).$$

The bank acceleration, $g \sin \phi$, can therefore be determined from this equation by substituting the estimate of the derivative of lateral velocity from the observer. This value is then low pass filtered, with the filter constant depending on the operating conditions.

$$g \sin \hat{\phi} = \left(\dot{\hat{v}}_y + v_x \Omega - a_{ym} \right)_{filtered} \quad (18).$$

Here the hat denotes an estimate. Note that since the estimate of bank angle is filtered, it may occasionally lag behind the actual bank angle, especially when the bank angle changes fast.

In principle, the bank angle could be compensated by adding the bank acceleration estimate to the right-hand side of the observer equation (6). This, however, has the following drawbacks: 1) bank estimate uses the estimate of side slip acceleration and vice versa, side slip estimate relies on the estimate of bank angle; this creates potential for divergence of both estimates in some situations; 2) the time lag in the bank angle estimate due to filtering is increased when the bank angle is compensated for dynamically. This may lead to significant errors when bank angle changes quickly.

Consequently, it was selected to use the observer equation (6) without the bank effect to determine the initial side slip velocity estimate. The effect of bank angle is compensated for by subtracting from the initial estimate the term given by equation (15) representing the steady-state bias due to bank. The bank angle estimate uses the estimate of side slip acceleration derived from the dynamic observer equation, without bank compensation. This approach avoids both problems associated with the dynamic approach. The bank compensation term, however, depends on the values of cornering stiffness per axle, which vary with operating point of vehicle. To improve the estimation, these values are adjusted depending on the operating point of vehicle and tires. This quasi-static bank compensation proved more robust than the dynamic approach.

Vehicle Testing

Vehicle testing was performed on three surfaces: dry asphalt, snow and ice using a variety of maneuvers and vehicle speeds. Initially, vehicle test data was used to develop and validate vehicle model in CarSim for simulation. It was found that scaling down the tire characteristics obtained on dry surface by the surface friction coefficient and applying them to snow or ice, as is commonly practiced, did not produce a good match between simulation and test data in these conditions. This is primarily because the shapes of these characteristics on different surfaces change in a manner that is different than that modeled by the tire characteristics used by CarSim. This is especially true for the data corresponding to the large longitudinal or lateral slips. On some surfaces the tire forces continue to rise as slip increases, on others they reach a peak and

then decline. Therefore distinct tire force characteristics were used for each surface.

Analysis of speed data indicated that in maneuvers in which vehicle remained stable and the ABS and TCS systems were enabled, the errors in vehicle speed did not exceed 2 kph or 3%, whichever is greater, for any significant period of time. As expected, within the above limitations, the estimates were the worst on ice, especially during braking or when vehicle slip angle was large. (Of course the estimate deteriorated when ABS or TCS systems were disabled, but then ESC would also be disabled).

Preliminary test evaluation of the side slip estimation algorithm was designed to detect potential problems. Therefore, the main focus was on maneuvers and conditions presenting difficulties in estimation. A significant portion of testing was performed on low friction surfaces, where lateral acceleration and sometimes yaw rate are often low in magnitudes, which may lead to significant error to signal ratios. Figure 5 shows one example of a vehicle test result for a lane change maneuver on a snow surface at 60 kph with ESC disabled. A Datron optical speed sensor was used to measure the actual side slip angle for comparison to the estimate. The data shows close correlation of the estimate and the measurement.

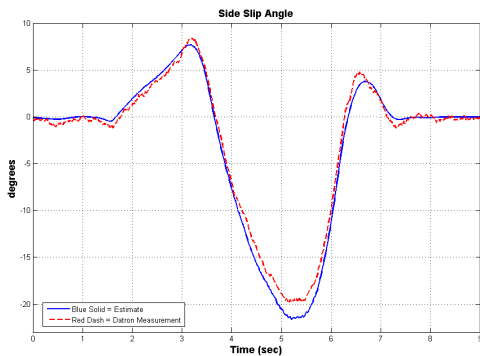


Figure 5. Vehicle test data for lane change maneuver on snow at 60 kph.

Many test maneuvers included a steady-state portion where the effect of errors may be integrated over time. Testing on banked surfaces was limited due to safety concerns. Parameters of vehicle were subjected to variations through changes in weight distribution, tire pressure variation between front and rear axle, changes in type of tires, acceleration and

deceleration during maneuvers and trailer towing. Overall, the test results demonstrated very good performance and robustness of the side slip estimation algorithm. One notable exception were a few instances of maneuvers performed on snow when the surface estimate did not drop early enough, resulting in under estimation of slip angle. As a result, improvements in the surface estimation algorithm were made.

One example of evaluation of robustness of the algorithm is testing performed with a 5000 lb trailer. The test vehicle with a trailer is shown in Figure 6.



Figure 6. Test vehicle with a trailer.

The presence of the trailer results in a hitch force at the rear of vehicle, which is not accounted for in the model and may have significant lateral component during cornering maneuvers. Hence, a significant deterioration of the quality of estimates in the presence of trailer was expected. This concern proved to be unjustified. A representative example of test results is shown in Figure 7, where the estimates of vehicle speed, side slip angle and road bank angle are shown.

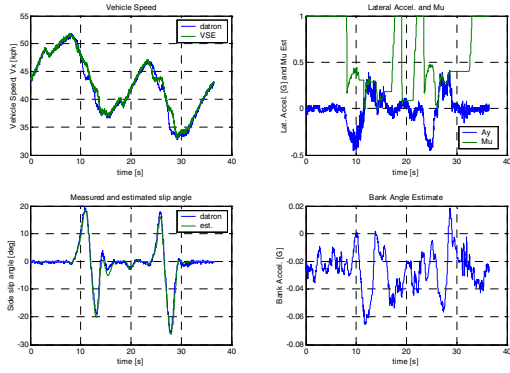


Figure 7. Estimates of vehicle slip angle, speed and road bank angle for vehicle with trailer during lane changes on snow.

In this severe maneuver, the estimate of side slip angle tracks the actual value very well, even at the side slip angle exceeding 20 degrees. The speed estimate is accurate most of the time with deviations occurring during relatively short periods of time when vehicle side slip angle is large. The estimate of bank angle is small throughout this maneuver performed on level surface. In other maneuvers with the trailer, including steady-state maneuvers, the estimator of side slip angle also performed very well, contrary to initial expectations. The main reason for this good performance is that even though the unknown lateral force at the hitch point is not explicitly used by the estimator, it is reflected in the measured yaw rate and lateral acceleration, which are both used in the estimation. In severe transient maneuvers, when the lateral force at the hitch tends to be large, the yaw rate of the vehicle is also significant and changing fast, which provides enough feedback to the observer to render the estimation error small due to this force disturbance. During steady-state maneuvers, on the other hand, when the presence of un-modeled lateral force at the hitch could lead to significant error due to integration, the lateral force is small. This can be shown using a free-body diagram of vehicle with trailer in Figure 8.

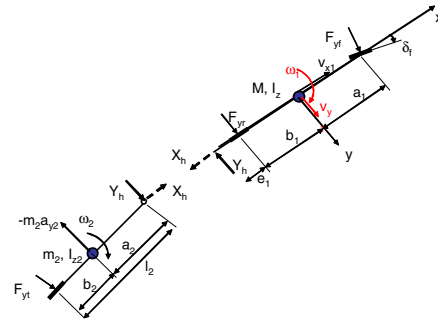


Figure 8. Simple model of vehicle with trailer.

If the hitch angle is small, then the lateral force at the hitch, Y_h , in a steady state turn is

$$Y_h = m_2 \frac{b_2}{l_2} a_{y2} \quad (19).$$

Here m_2 denotes the total mass of the trailer, b_2 is the distance of the trailer center of mass to the trailer axle, l_2 the distance of the hitch point to the axle and a_{y2} is the lateral acceleration of the trailer. Since the distance b_2 is usually much smaller than l_2 , the lateral force at the hitch is much smaller than the inertial force $m_2 a_{y2}$. In the special case when $b_2 = 0$ (i.e. the trailer center of mass is directly above the axle), the lateral hitch force is 0 since the inertial force is fully balanced by the lateral tire force (without an unbalanced yaw moment). The effect of the lateral hitch force, Y_h , on the estimated side slip velocity can be evaluated analytically as described in the previous section for the bank angle. This yields the following value of the steady-state error in lateral velocity:

$$e_{v_{y,ss}} = -\frac{Y_h v_x}{C_f + C_r} = \frac{-m_2 b_2 a_{y2} v_x}{l_2 (C_f + C_r)} \quad (20).$$

Simulation

The most comprehensive evaluation of estimation robustness was performed through simulation using a validated vehicle model. Since the vehicle and the observer are non-linear systems, both performance and stability of the estimation algorithm depend on driver inputs, vehicle speed and environmental conditions, in particular the surface coefficient of friction. Simulations have been performed using different steering inputs, vehicle speeds and road surfaces. The set of handling maneuvers consisted

of five steering patterns: ramp steer, step steer, open loop lane change, slalom and fishhook. The steering amplitudes, rates of change and frequencies depended on the speed and surface friction. The following initial speeds of vehicle were used: 30, 50, 70, 120, 140 and 180 kph. Maneuvers were simulated on dry surface, snow and ice. Some combinations of steering amplitudes and initial speeds were eliminated, for example when the combination of speed, steering angle and surface friction resulted in vehicle being well within the linear handling range.

The individual factors contributing to the estimation errors were as follows:

- errors in lateral acceleration measurement, including bias and micro-gradient errors
- errors in yaw rate measurement, including bias and micro-gradient errors
- errors in estimated vehicle speed
- payload variations
- variations in tire characteristics, including cornering stiffness and ultimate grip
- variation in road bank angle
- variation in front/aft road inclination
- vehicle deceleration due to braking
- vehicle acceleration

For each of these factors, reasonable ranges of variations were estimated. For example, the ranges of sensor errors are known from specifications and the sensor test data. For the sensors considered here, the errors consist of two largely independent components: bias, which is an error when the measured signal is zero and micro-gradient error, which is an error due to changes in the scale factor, resulting in an error proportional to the magnitude of the measured signal. The range of errors is illustrated conceptually in Figure 9.

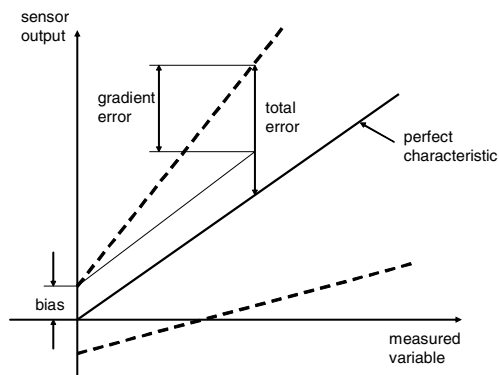


Figure 9. General sensor error characteristic.

Since the bias is constant or slowly varying, it can be partially compensated for most sensors. The errors in the steering angle are so small that they have no meaningful effect on side slip estimation and are not considered. For other contributing factors, the range of variations was selected based on experience. In the case of bank angle, the maximum angle of 20 degrees was used. While the road grade on public roads is limited to 12%, which corresponds to bank angle of about 7 degrees [8], larger bank angles are possible when vehicle leaves the road. For obvious reason a lower value was assumed on ice.

First, simulation study was performed using only single factors defined above. Note that in the case of sensor errors, a “single factor” here means a combination of both bias and micro-gradient errors. In each case the maximum errors or parameter variations from both sides of the spectrum were considered. For each contributing factor a variety of maneuvers on different surfaces, amplitudes of the steering angle and entry speeds were used. Representative simulation results are discussed next.

In Figure 10 the results of simulations for a Fishhook maneuver performed at 90 kph on dry surface are shown with variations in the tire cornering stiffness as an error-contributing factor. Two extreme cases are shown: 1) front stiffness reduced by 20% and rear stiffness increased by 20% compared to nominal values and 2) vice versa, that is front stiffness increased by 20% and rear stiffness reduced by 20%. In the first case the vehicle develops significantly smaller, and in the second much larger side slip angle than the nominal vehicle. In spite of very large difference in the slip angles between the two extremes, the side slip angle estimator tracks the actual slip angle very well in both cases.

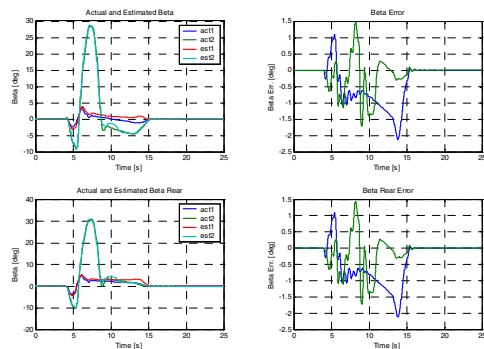


Figure 10. Estimation of slip angle in a Fishhook maneuver performed with tire cornering stiffness variations: 1) -20% front, +20 rear, 2) +20 front - 20 rear vs. nominal.

In Figure 11 the results of simulations in an aggressive lane change on snow at 70 kph are shown. The error factor was the road inclination: in the first case the road was flat, in the second there was -10 degree (e.g. downhill) inclination. In the first case the vehicle remained stable, in the second it spun out, yet the observer tracks the actual slip angle in both instances. In the case of vehicle spin out, the absolute error of estimation is quite small when the slip angle is below 15 degrees; after that it is underestimated.

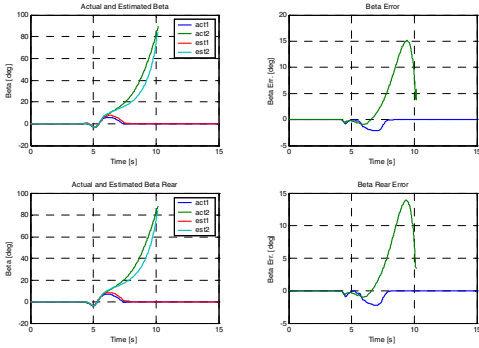


Figure 11. Side slip angle in a lane change maneuver on snow without and with 10 degree road inclination.

As a result, the influence of each factor on the side slip angle estimation error was quantified in terms of average increase in estimation error over the entire set of maneuvers and in terms of maximum increase in estimation error for all maneuvers without spin outs. The former result is summarized in Figure 12.

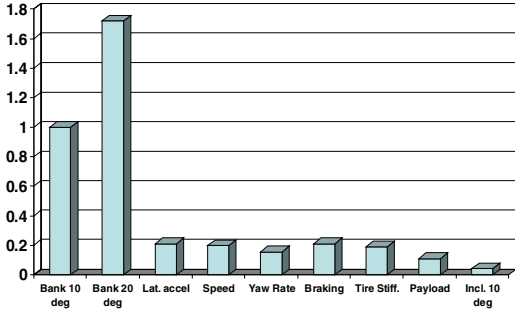


Figure 12. Average maximum increases in estimation errors due to individual factors (effect of 10 degree bank corresponds to 1).

The bank angle of the road has the largest contribution to the side slip estimation error, while road inclination and payload variations have relatively modest influences. The remaining factors have medium effect on average, but they may differ substantially among maneuvers.

In addition to the magnitudes of the estimation errors, the direction of the side slip angle error resulting from each individual factor were determined. These findings were confirmed by simplified analysis and are summarized in Table 1.

Factors contribute to over-estimation either because the estimate increases more than the actual vehicle response or the vehicle response decreases more than the estimate. An analogous statement is true in the case of under-estimation tendency. One possibly surprising result is that both heavy braking and heavy acceleration usually contribute to overestimation. Braking has primarily two effects, which have opposite influences on the vehicle slip angle. It increases the front axle normal load, which tends to increase front lateral force and the vehicle slip angle. Braking also introduces longitudinal slip of front and rear wheels, which reduces lateral forces. During heavy braking the brake slip of the front wheels is significantly larger than that of the rear wheels, which decreases vehicle slip angle. Under heavy

braking, the second effect is typically larger than the first, hence vehicle slip angle is reduced as compared to the case without braking, leading to overestimation tendency.

Table 1. Single factors contributing to over- and under-estimation of side slip

Factor contributing to side slip over-estimation	Factor contributing to side slip under-estimation
Bank angle in the direction that reduces measured lateral acceleration	Bank angle in the direction that reduces measured lateral acceleration
Lateral acceleration errors reducing the magnitude of lateral acceleration	Lateral acceleration errors increasing the magnitude of lateral acceleration
Yaw rate errors increasing the magnitude of yaw rate	Yaw rate errors reducing the magnitude of yaw rate
Vehicle speed errors increasing the magnitude of speed	Vehicle speed errors reducing the magnitude of speed
Heavy braking (usually)	
Reducing front tire cornering stiffness and increasing rear cornering stiffness	Increasing front tire cornering stiffness and reducing rear cornering stiffness
Front payload bias	Rear payload bias
Uphill road inclination	Downhill road inclination
Heavy acceleration (usually)	

During acceleration, the normal load of the rear axle is increased, which increases lateral force capability and reduces vehicle slip angle. At the same time longitudinal slip on driven wheels is present, which reduces the lateral force capability of these wheels. For front wheel drive vehicle, this further contributes to the reduction in side slip angle, for the rear wheel drive it increases the side slip angle, but for vehicle with traction control this increase usually does not

dominate the first effect. Thus in most cases heavy acceleration reduces side slip angle as compared to the case without acceleration.

After studying the effect of single factors, the effect of multiple factors was considered. In order to reduce the number of cases to a manageable level, only the worst cases were considered. Based on the single factor study, the worst combinations of multiple factors were determined. The underlining principle was to stack up the factors, which have the largest effect on estimation error and act in the same direction. When two or three factors were considered, the extreme errors were used for each one of them in the direction that produce the estimation error in the same direction. However, since most of the factors can be considered independent random variables, stacking up the maximum errors of more than three factors is too conservative. As the number of factors increases, it becomes increasingly unlikely that each one of them is at the extreme of the range. In order to keep the same confidence level in the case of multiple factors as for single factors, the maximum errors for each factor in the multiple-factor analysis, $e_{\max i}^{mult}$ is

$$e_{\max i}^{mult} = e_{\max i}^{ind} / \sqrt{N-1} \quad (21).$$

Here $e_{\max i}^{ind}$ is the maximum error used in the single factor analysis and N is the number of contributing factors in the multiple factor analysis.

Two important findings of the robustness analysis were that the single largest factor contributing to errors in side slip estimate was a large bank angle of the road. At the same time, it was observed that the bank angle estimates were quite reliable. Consequently two ways of increasing robustness have been pursued: improvement in compensation for bank angle during estimation and gradually eliminating side slip angle control when very large bank angles are detected.

CONTROL SYSTEM ROBUSTNESS

By definition, the robustness of a system is related to its sensitivity to parameter variations. A fundamental advantage of a closed loop control system is its ability to have low sensitivity, i.e. high robustness, to internal variations. For vehicle handling control systems, typical variations are due to changes in tires, load conditions, sensors, road friction, speed, and others. To verify the robustness

of the entire control system, an extensive analysis was performed to evaluate the impact of internal variations along with input variations.

The control system robustness analysis consisted of two phases. The intent of the first phase was to provide exposure to a wide variety of maneuvers on several road surfaces and various speeds. Both vehicle tests and simulations were used in this phase. The variable elements included driver inputs (steering, braking, and throttle), surface coefficient of friction, and vehicle speed. The other vehicle parameters were held constant at nominal values throughout this analysis phase. The test matrix is shown in Table 2.

Table 2. Test matrix for phase 1

#	Maneuver	Method	Speeds	Road Friction Coefficient
1	Ramp Steer	Simulation	50,75,100 MPH 50,75,100 MPH 25,50,75 MPH	@ 1.0 @ 0.3 @ 0.1
2	Constant Radius, Increasing Speed	Vehicle Test	Ramped to Max	@ 1.0 @ 0.3 @ 0.1
3	Step Steer With Reversal	Simulation	50,75,100 MPH 50,75,100 MPH 25,50,75 MPH	@ 1.0 @ 0.3 @ 0.1
4	Fishhook	Simulation	35, 40, 45, 50 MPH	@ 1.0 @ 0.3 @ 0.1
5	Fishhook	Vehicle Test	35, 40, 45, 50 MPH	1.0
6	Sine-With-Dwell Lane Change	Simulation	50,75,100 MPH 50,75,100 MPH 25,50,75 MPH	@ 1.0 @ 0.3 @ 0.1
7	Sine-With-Dwell Lane Change	Vehicle Test	50 MPH	1.0
8	OEM-Spec Steer Profiles	Simulation	Per Spec	Per Spec
9	Driver-In-The-Loop Lane Changes	Vehicle Test	Per Spec	@ 1.0 @ 0.3 @ 0.1
10	Split-Mu Braking, Split-Mu Accel	Vehicle Test	2 Speeds Each	0.1 / 1.0
11	Combined Steer/Brake/Throttle	Vehicle Test	2 Speeds Each	@ 1.0 @ 0.3 @ 0.1

In the second phase of the control robustness study, sensitivity to variations in vehicle parameters, sensor errors, and variations in environment was evaluated. Simulation analysis was a primary approach used in this phase. The evaluation was performed after the side slip estimation robustness analysis was completed, and it proceeded along the same lines. One exception was that in order to reduce the total number of simulations, only the worst among the

single factors and the worst combinations of multiple factors were considered. Specific maneuvers were limited to the ramp steer, step steer, fishhook, and sine-with-dwell lane change.

As intended, the overall process to design and tune the control algorithm and to evaluate its robustness was an iterative sequence. In the first iteration, the results of the phase 1 analysis showed the need to make improvements through tuning and through some minor algorithmic modifications. After modifications were implemented, the robustness analysis was repeated to confirm the improvements. Specifically improvements were made in the way the feedback and feed-forward control terms are merged to form the total yaw moment command. Still other improvements were made in the surface friction estimation algorithm.

The following figures show representative data from vehicle tests and from simulations as part of the robustness analysis. Figure 13 shows a vehicle test result for a sine-with-dwell lane change maneuver at 50 MPH on dry asphalt, with overlay comparison for ESC Off and On. A steering robot was used to generate the NHTSA-specified steer input [9]. Comparing the results, the side slip angle is held to an appropriately small magnitude and the yaw rate and lateral acceleration decay more quickly with ESC On, indicating an improvement in the stability margin.

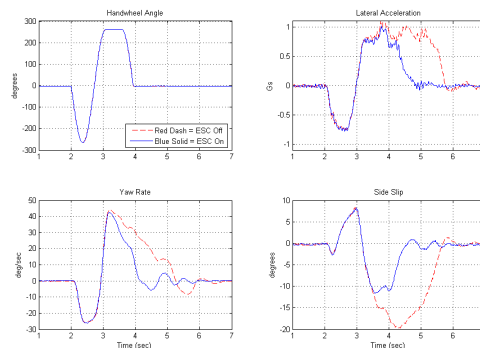


Figure 13. Vehicle test data for sine-with-dwell lane change maneuver at 50 MPH

Figure 14 shows a simulation result for a step-steer maneuver at 50 MPH on snow, with overlay comparison for ESC Off and ESC On. With ESC On, the side slip angle is well regulated and the vehicle's handling response is stable. With ESC Off, the side slip angle diverges quickly which indicates a

spin-out condition, demonstrating a loss of handling stability.

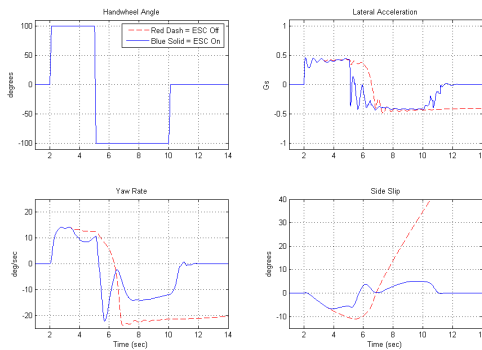


Figure 14. Simulation data for step steer maneuver at 50 MPH on snow

Lastly, in this investigation it was found that attenuating the side slip angle control on roads with large banks was very effective in improving robustness with respect to errors in side slip angle estimation in these conditions. Additionally it was found that the control was always appropriate when active, and the weighting factor worked very well to balance vehicle responsiveness (tracking of the desired yaw rate) versus stability (side slip angle control).

CONCLUSIONS

In this paper a systematic process of evaluating robustness of a side slip angle estimation and control algorithm has been described. The side slip angle estimator is a nonlinear reduced order observer with compensation for road bank angle. The control algorithm combines tracking control of vehicle yaw rate with regulation of rear axle side slip angle and blends these tasks smoothly depending on the operating conditions. Evaluating robustness of the algorithm was an iterative process, in which initial results of robustness investigation provided motivation for improvements in algorithms providing sensor bias compensation, road bank angle compensation, surface friction estimation and blending of control terms. Robustness was evaluated using a set of maneuvers performed at different speeds and different surface conditions. The effects of single error-contributing factors on estimation errors was first evaluated. This provided information regarding the magnitude and direction of errors

resulting from single factors, which in turn was used to identify the worst combinations of factors for multiple factor evaluation. The study involving multiple factors was reduced to the worst case scenarios, which helped keep the number of combinations manageable. Modifications in the control laws were made to maintain robustness in rare conditions when the side slip angle estimation error could be significant due to large bank angle.

REFERENCES

- [1] Koibuchi, K., Yamamoto, M., Fukuda, Y., and Inagaki, S., 1996, "Vehicle Stability Control in Limit Cornering by Active Brake", SAE paper No. 960487.
- [2] You, S., Yoo, S., Hahn, J.-O., Lee, H., and Lee, K.L., 2006, "A New Adaptive Approach to Real-Time Estimation of Vehicle Side slip and Road Bank Angle", Proceedings of 8-th International Symposium on Advanced Vehicle Control (Taipei, Taiwan, August 20-24). 427-432.
- [3] van Zanten, A. T., 2000, "Bosch ESP: 5 Years of Experience", SAE paper No. 2000-01-1633.
- [4] Sasaki, H. and Nishimaki, T., 2000, "A Side-Slip Angle Estimation Using Neural Network for a Wheeled Vehicle", SAE paper No. 2000-01-0695.
- [5] Fukuda, Y., 1999, "Slip-Angle Estimation for Vehicle Stability Control", Vehicle Systems Dynamics, Vol. 32, pp. 375-388.
- [6] Nishio, A., Tozu, K., Yamaguchi, H., Asano, K., Amano, Y., 2001, "Development of Vehicle Stability Control System Based on Vehicle Side slip Angle Estimation", SAE paper No. 2001-01-0137.
- [7] Forkenbrock, O'Harra, Elsasser, 2004, A Demonstration of the Dynamic Tests Developed for NHTSA's NCAP Rollover Rating System - Phase VIII of NHTSA's Light Vehicle Rollover Research Program, DOT HS 809 705
- [8] "A Policy on Geometric Design of Highways and Streets," AASHTO, 1994
- [9] NHTSA Proposed Rule for FMVSS 126, U.S. Federal Register Vol. 71, No. 180, September 18, 2006